Evaluation of a Variable Mixing Efficiency Parameterization on the Simulation of Last Glacial Maximum (LGM) Oceanic Circulation

by

Danil Thorstensson

A THESIS

submitted to

Oregon State University

Honors College

in partial fulfillment of
the requirements for the
degree of

Honors Baccalaureate of Science in Earth Sciences and Environmental Economics and Policy
(Honors Associate)

Presented June 1, 2021
Commencement June 2021

AN ABSTRACT OF THE THESIS OF

Danil Thorstensson for the degree of Honors Baccalaureate of Science in Earth Sciences and Environmental Economics & Policy presented on June 1, 2021. Title: Evaluation of a Variable Mixing Efficiency Parameterization on the Simulation of Last Glacial Maximum (LGM) Oceanic Circulation.

Abstract approved:_____

Andreas Scmittner

This study tested the utility of a variable mixing efficiency formulation proposed by Mashayek, et al. (2017) for use in oceanographic models other than the modern, pre-industrial ocean. This formulation is used to calculate diapycnal (vertical) mixing due to unresolved subgrid-scale processes. Results from Last Glacial Maximum (LGM) simulations for variables such as sea surface temperature, density, and meridional overturning were compared to those of a model simulation of the pre-industrial ocean using three different parameter conditions for mixing efficiency and one "default" constant value of $\Gamma = 0.2$. These three parameter conditions were influenced by Mashayek, et al. (2017), who devised a variable mixing efficiency parameterization and applied it to the pre-industrial ocean. Simulated changes in meridional overturning between the pre-industrial and LGM simulations were very similar for the constant mixing efficiency coefficient models and the variable coefficient models; e.g. the flow of North Atlantic Deep Water out of the Atlantic was ~2 Sv less in the LGM simulations for both variable and constant Γ models.

The null hypothesis that a variable mixing efficiency parameterization would not significantly affect differences in physical variables between LGM and pre-industrial simulations was not rejected. A constant Γ is recommended for future modeling of the ocean-climate system.

Key Words: mixing efficiency, ocean, turbulence, diapycnal diffusivity, Last Glacial Maximum, pre-industrial, Buoyancy Reynolds number

Corresponding e-mail address: danil.thorstensson@gmail.com

©Copyright by Danil Thorstensson

June 1, 2021

Evaluation of a Variable Mixing Efficiency Parameterization on the Simulation of Last Glacial Maximum (LGM) Oceanic Circulation

by

Danil Thorstensson

A THESIS

submitted to

Oregon State University

Honors College

in partial fulfillment of
the requirements for the
degree of

Honors Baccalaureate of Science in Earth Sciences and Environmental Economics & Policy
(Honors Associate)

Presented June 1, 2021

Commencement June 2021

Honors Baccalaureate of Science in Earth Sciences and Environmental Economics & Policy project of Danil Thorstensson presented on June 1, 2020.

APPROVED:

_____

Andreas Schmittner, Mentor, representing CEOAS

_____

Karen Shell, Committee Member, representing CEOAS

_____

William Smyth, Committee Member, representing CEOAS

_____

Toni Doolen, Dean, Oregon State University Honors College

I understand that my project will become part of the permanent collection of Oregon State University, Honors College. My signature below authorizes release of my project to any reader upon request.

_____

Danil Thorstensson, Author

INTRODUCTION

Deep-sea oceanic circulation is in large part driven by the breaking of internal waves and turbulent mixing as a result of the deflection of currents by underwater topography (e.g. MacKinnon et al., 2017). Therefore, the study of oceanic circulation relies on accurate measurements and modeling of turbulent mixing. Mathematical descriptions (parameterizations) of turbulent mixing involve the mixing efficiency coefficient (the non-dimensional variable Γ), which quantifies the proportion of the energy available from turbulence that is expended in mixing across density surfaces (Mashayek, et al., 2017) and contributes to diapycnal diffusivity (Gregg, et al., 2018). Previous modeling of diapycnal, or vertical, oceanic mixing has mostly assumed a constant Γ of 0.2 as an approximation of the average mixing efficiency, which ignores spatial and temporal variations although it may still be a good approximation in many situations (Smyth 2020).

In order to make up for this potential over-simplification, Mashayek, et al. (2017) have investigated the merits of a variable mixing efficiency coefficient, using a formula that allows for differences in oceanic conditions. However, the variable mixing efficiency formulation by Mashayek, et al. (2017) has not yet been tested in historical global oceans, which is the goal of this study. Mashayek, et al. (2017) suggested using lower and upper bounds to account for the uncertainty associated with estimating variable mixing efficiency. Here we consider this uncertainty by using three different parameter combinations, *lower, middle,* and *upper*, corresponding to variable mixing coefficients that were varied to account for topographical and geographical differences (e.g., the *upper* parameter models mixing that occurs in areas of the ocean with greater energy expended into mixing). These three parameter combinations were then

compared to simulations with a "*default*" coefficient of $\Gamma = 0.2$. (*Default, lower, middle,* and *upper* in italics will hereafter be used in reference to the different parameterizations that were used in simulations.)

Research with a variable mixing efficiency as of yet has only been conducted for the modern ocean (see Mashayek, et al., 2017). Climate models with constant mixing efficiency have been applied to model past ocean conditions including changes in mixing (e.g. Wilmes et al., 2019). The question arises whether those results are robust or whether they need to be revised due to changes in mixing efficiency. Here we will address this question by comparing results of the variable mixing efficiency parameterization with results using a constant value in simulations of the Last Glacial Maximum (LGM), roughly 20,000 years ago, and the pre-industrial ocean.

The null hypothesis is that the variable mixing efficiency parameterization will not significantly affect changes between the LGM and pre-industrial simulations. If the results show that the variable Γ influences the difference between the preindustrial and LGM oceans, this could suggest that it may also influence results for other historical oceans, for use in paleoclimate, for example. It could also suggest that a variable Γ can be used for oceans of the future, potentially for use in the modeling of the impacts of climate change in the 21st century and beyond.

DATA, MODEL, & METHODS

This analysis used the Oregon State University version of the University of Victoria (OSU-UVic) Earth System Climate Model (see Weaver, et al., 2010), which is a climate model of intermediate complexity with a three-dimensional general circulation ocean model. The model is coupled to a

thermodynamic/dynamic sea-ice model, a single layer energy-moisture balance atmospheric model, and a land surface and dynamic vegetation model. It also includes an ocean ecosystem and biogeochemistry model, but these components were not used for the study. As expressed in Schmittner & Egbert (2014), model components use a resolution of 3.6° longitude and 1.8° latitude and the ocean is divided into 19 vertical levels, with grid spacing that increases from 50 m near the surface to 500 m near the ocean floor. Ocean mixing and diffusivity were parameterized as described in Schmittner & Egbert (2014) to consider scales too small to be resolved by the coarse-resolution model grid.

In order to test the effect of different mixing parameters, different parameters were created for use in the equation $\Gamma = 2\Gamma^*(Re_b/Re_b^*)^{1/2} / (1+Re_b/Re_b^*)$, which measures the effects of changes in deep-sea conditions on the mixing efficiency coefficient Γ. An equivalent representation for Γ is $\Gamma = \eta/(1-\eta)$, where η is the ratio of the rate of energy spent on irreversible mixing to the total energy available to turbulence. The buoyancy Reynolds number ($Re_b = \epsilon/\nu N^2$), according to Mashayek, et al. (2017), refers to the "ratio of the tendency of turbulence to mix density vertically (ϵ) to the combined influence of density stratification (N^2) and viscosity (ν) in suppressing vertical motion and turbulence." The buoyancy Reynolds number is often seen as a "measure of turbulence 'intensity'" (Mashayek, et al., 2017). Re_b^* represents the buoyancy Reynolds number at which Γ peaks. Since its value is uncertain we have chosen different values for this study, described below. The second uncertain parameter is Γ* which specifies the maximum mixing efficiency for a given buoyancy Reynolds number (Mashayek, et al., 2017).

The Γ* and Re_b^* values chosen for this study correspond to buoyancy Reynolds numbers ranging from 100 to 300 and maximum variable mixing efficiencies of 0.2 to 0.5 at a given Re_b.

This translated into one "*lower*" parameter condition of (Re_b*, Γ*) = (100, 0.2), one "*higher*" parameter of (300, 0.5), and one right in the "*middle*" of these two, at (200, 0.35). These parameter conditions were chosen because they roughly corresponded to lower and upper bounds for these values in the literature, as discussed by Mashayek, et al. (2017). The "control" simulations use a constant Γ = 0.2, which is an approximated value common in the literature. This parameterization yields maximum values for Γ in the ocean interior and smaller values towards the surface and sea floor (Fig. 3 in Mashayek et al., 2017), consistent with the idea that mixing is less efficient close to the boundary layers (Smyth, 2020).

Updated ice sheet reconstructions and wind stress data were added into the UVic model for the LGM simulations as described in Muglia, et al. (2018). This change is in light of new research more conclusively showing the increases in wind shear and diffusivity in the LGM ocean (e.g. Sherriff-Tadano, 2017). A 4,000 year spin-up was conducted to ensure that an equilibrium in the ocean was reached before the historically-forced simulations got underway.

RESULTS

MERIDIONAL OVERTURNING

Meridional Overturning Pre-Industrial

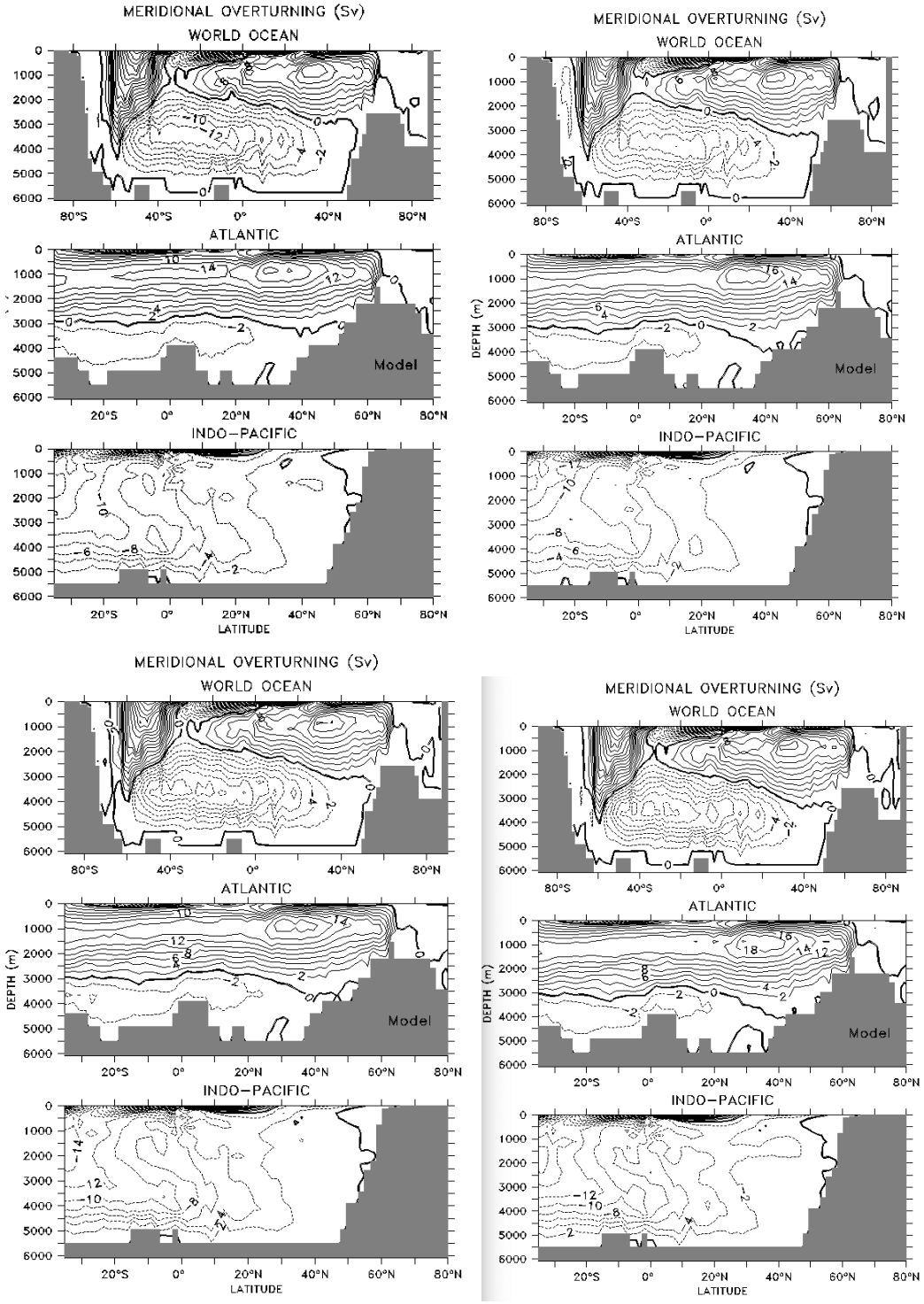

Figure 1. Pre-Industrial Meridional Overturning (clockwise/conter-clockwise flow is indicated by solid/dashed lines): Default (top left), Lower (top right), Middle (bottom left), Upper (bottom right). 1 Sv = 10^6 m^3/s.

The largest differences in Meridional Overturning Circulation (MOC) between the different simulations are seen in the Indo-Pacific Ocean, particularly in the southern hemisphere. The influx of water from the Southern Ocean below ~3,000 m is enhanced in the *upper* parameter setting and reduced in the *lower* case. This is consistent with the larger diapycnal diffusivities expected in the *upper* case: larger diapycnal mixing has been shown in the literature to lead to stronger MOC (e.g. Wilmes et al. 2019).

As for the Atlantic Ocean, the differences between the different parameterizations are less stark, with the *default* parameter set not being dramatically different from any of the variable mixing efficiency parameter sets (the output for *default* most resembled *lower* for this ocean, as it did for the output of the World Ocean). The inclusion of variability in mixing efficiency seems not to have made much of a difference in the simulation of the Atlantic. In general, for all oceans, the effect size for this variable is not particularly large, suggesting that a variable mixing efficiency is perhaps less essential for modeling meridional overturning in the pre-industrial ocean.

Meridional Overturning LGM

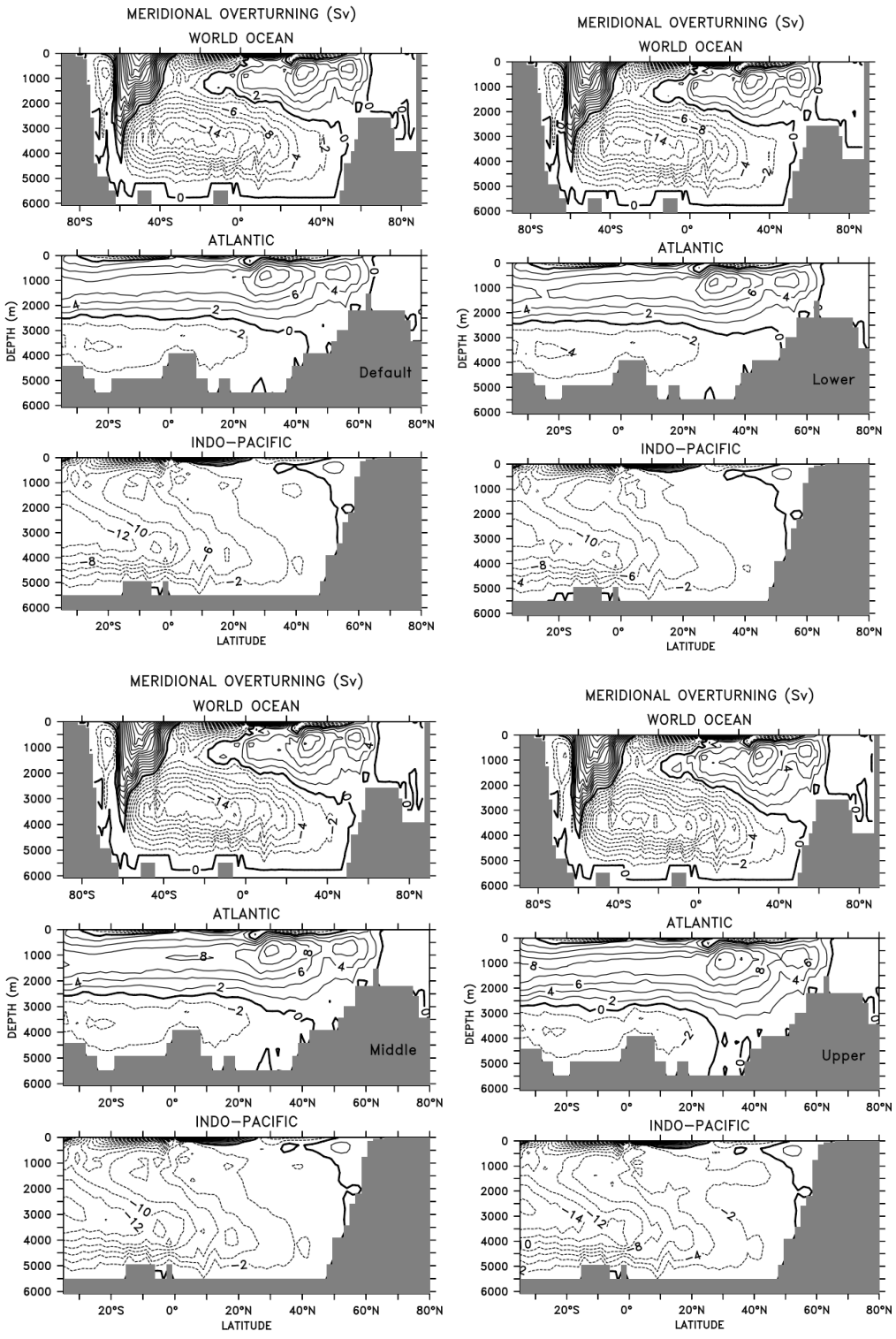

Figure 2. LGM Meridional Overturning (clockwise/conter-clockwise flow is indicated by solid/dashed lines): Default (top left), Lower (top right), Middle (bottom left), Upper (bottom right)

Overall, the differences between the variable and default parameter conditions for meridional overturning for the Last Glacial Maximum were minimal, although the differences between the upper and lower parameterizations can be seen in parts of the ocean. The circulation using the default parameterization proved to be most similar to the *lower* variable mixing efficiency simulation, both in the Atlantic and in the Indo-Pacific, with almost identical stream functions. In contrast, the *middle* and *upper* simulations result in stronger and slightly deeper Atlantic Meridional Overturning Circulations, slightly weaker Antarctic Bottom Water flow into the Atlantic, and increased inflow into the Indo-Pacific. However, those differences are relatively small (< 2 Sv; 1 Sv = 10^6 m^3s^{-1}).

DENSITY:

Density Pre-Industrial Results:

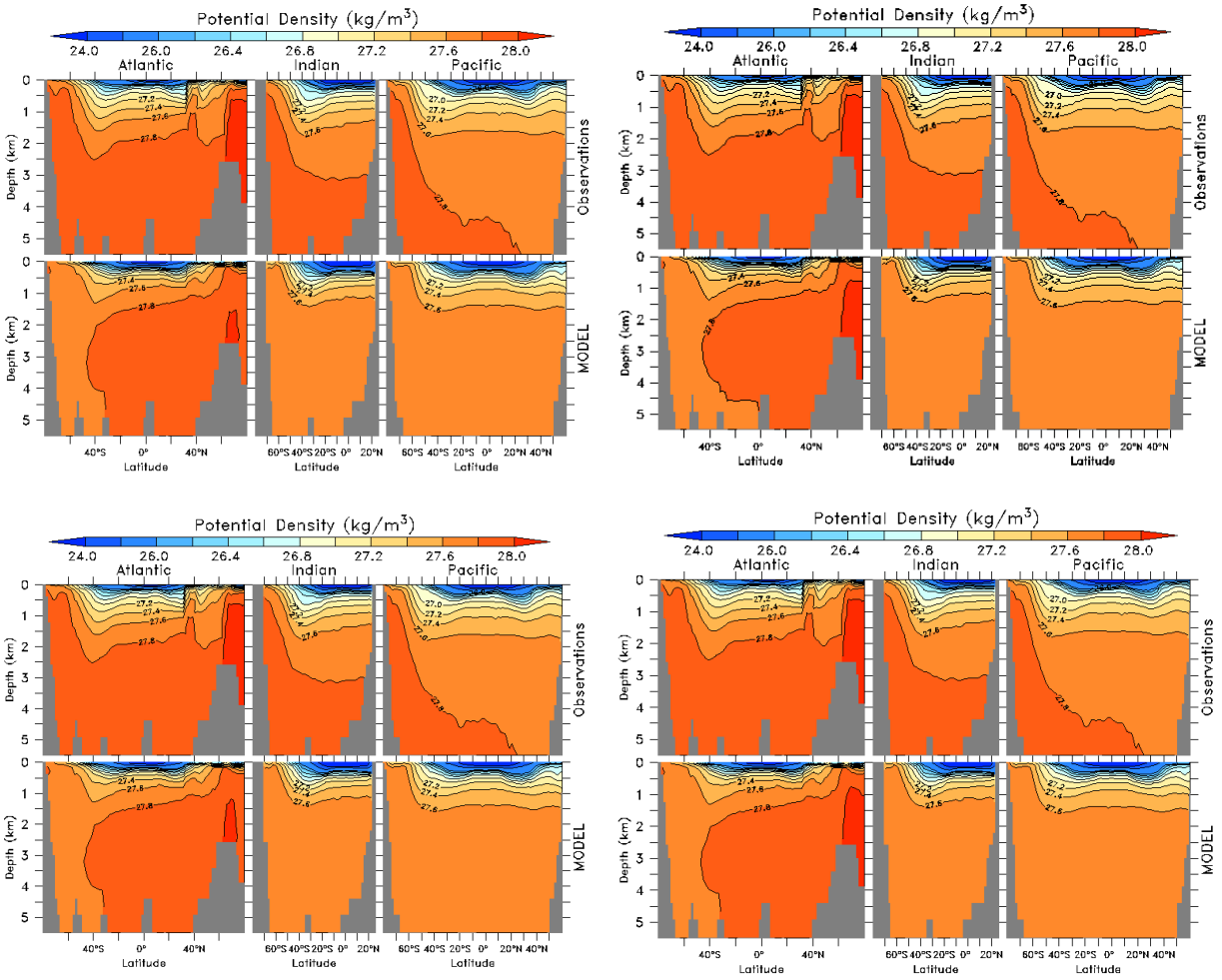

Figure 3. Pre-Industrial Potential Density (kg/m^3): Default (top left), Lower (top right), Middle (bottom left), Upper (bottom right). [Observations in top panels; Model results in bottom panels]

Figure 3 (above) shows the output of potential densities for all four parameter combinations in the pre-industrial ocean. The most striking difference between these different parameterizations is seen in the North Atlantic, corresponding to the branch of AMOC that is descending from the surface in the waters off of Greenland. Comparing the *default* output (top right in Figure 3) with the three variable parameterizations, it is clear that for this part of the ocean, the *middle*

parameterization (bottom left) is closest to it while both *lower* (top right) and *upper* (bottom right) show larger densities. This output, where the lower and upper extremes are close to one another and different from the parameter combination in the middle of them, is difficult to explain. With the greater intensity of mixing in the *upper* parameterization, it makes sense that the meltwater, and therefore the increase in density, is able to reach more of the ocean depths in the North Atlantic, but it is unclear what makes the *lower* parameterization output greater mixing effects than both *default* and *middle.* Regardless, it is clear that the *upper* and *lower* result in larger density gradients in the ocean overall, particularly in the North Atlantic, which has the effect of helping increase the strength of AMOC.

Comparing the results for all four parameterizations to the observations, *upper* and *lower* both better represent the real world than the *default* parameterization, primarily in the North Atlantic. All three "variable" parameterizations represent the Southern Ocean roughly the same, outputting a density of ~27.6 kg/m^3 for this region. The one difference between the three parameters is that *lower* shows slightly lower densities in the deep Southern Ocean and South Atlantic around a depth of 4-5 km. For the Pacific and Indian oceans, there is very little difference between the parameters, likely in part because of the decreased role of underwater topography in oceanic mixing and the lack of a strong circulation cell on the level of AMOC, which may accentuate differences between results.

A notable difference between the observations and the model output for all parameter combinations is that the model underestimated potential density for much of the deep ocean. In the observations, density is roughly 0.2 kg/m^3 higher in much of this region, particularly in the southern hemisphere. Although this is not a severe difference with observations, this suggests

that the model did not perfectly represent the effects that melting Antarctic ice shelves and sea ice has on the physical characteristics of sea water, in this context having to do with its salinity and temperature. Although much of the ocean below 2 km was modeled in line with observations, the lower modeled densities in the Southern Ocean perhaps suggest that the decreased oceanic temperature in this region due to ice melt were underestimated.

Density LGM:

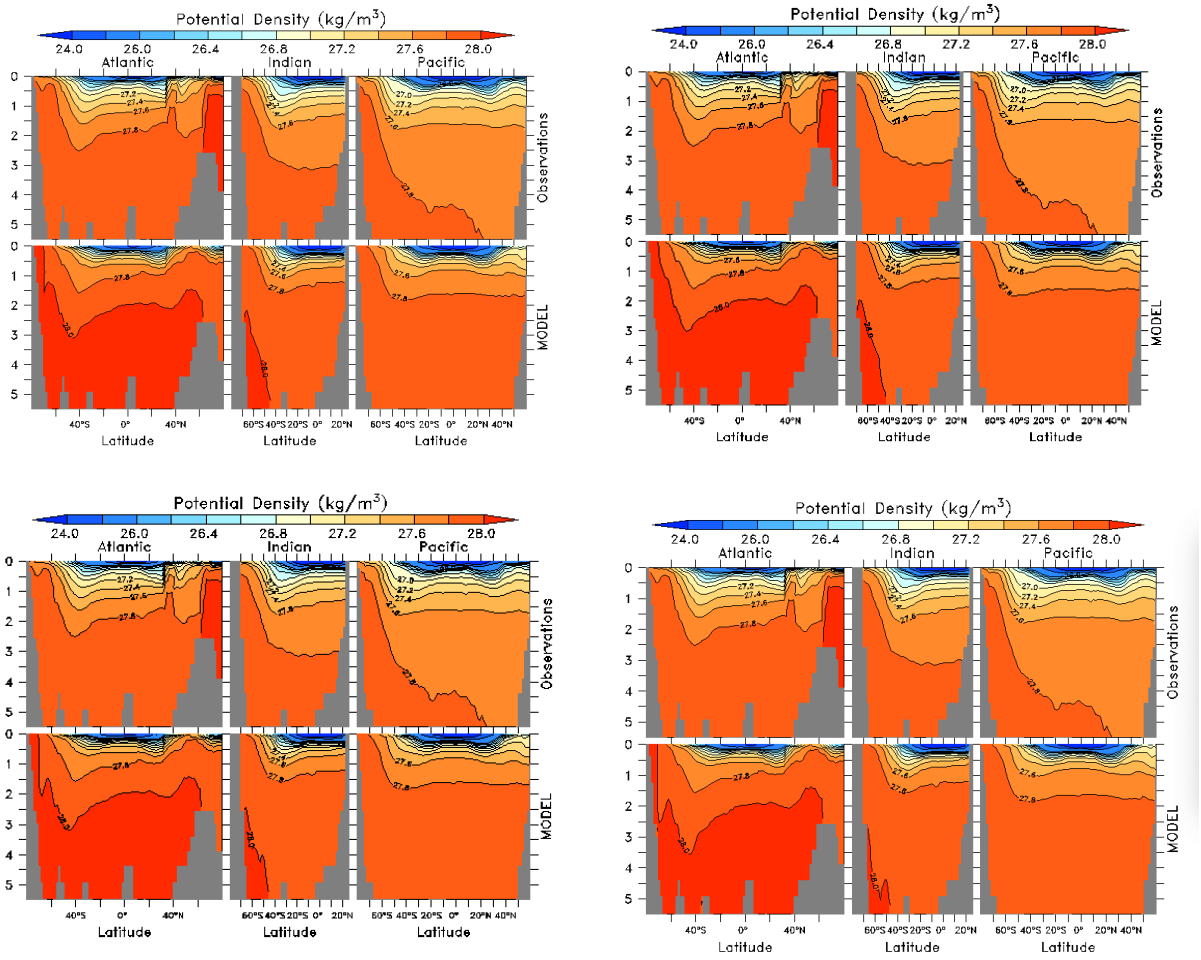

Figure 4. LGM Potential Density (kg/m^3): Default (top left), Lower (top right), Middle (bottom left), Upper (bottom right)

Figure 4 shows the density of the different parameterizations for the LGM ocean. For larger parameters (e.g., *upper*, in the bottom right), density at a given depth is slightly lower than for lower ones (e.g., *lower*, in the upper right). This is noticeable in the Indian Ocean and much less so in the Atlantic and Pacific. The explanation for this slight variation in the Indian Ocean could be that for greater mixing efficiencies, mixing is enhanced, which reduces stratification.

One interesting finding is that with the *default*, *upper* and *middle* parameterizations for the Southern Ocean, the gradation between greater and lower pressure (the boundary between 28 kg/m^3 and 27.8 kg/m^3, as Figure 4 shows) does not linearly decrease with depth, as it does with the *lower* results. Instead, there is a small hitch at a depth of roughly 1.5-2.5 km. Considering that the default parameters typically yield results in the range of *middle* and *upper,* this seems to be an output peculiar to higher levels of mixing efficiency. On the other hand, the output for the *lower* simulation, which shows a steady, nearly linear border between denser and less-dense ocean, suggests a role for the lower mixing efficiency. Lastly, there are imperceptible differences between the different parameters in the Pacific Ocean, as with the pre-industrial Pacific Ocean, because ocean mixing is less influential in its waters than for the other oceans and especially for the Atlantic.

TEMPERATURE:

Temperature Pre-Industrial:

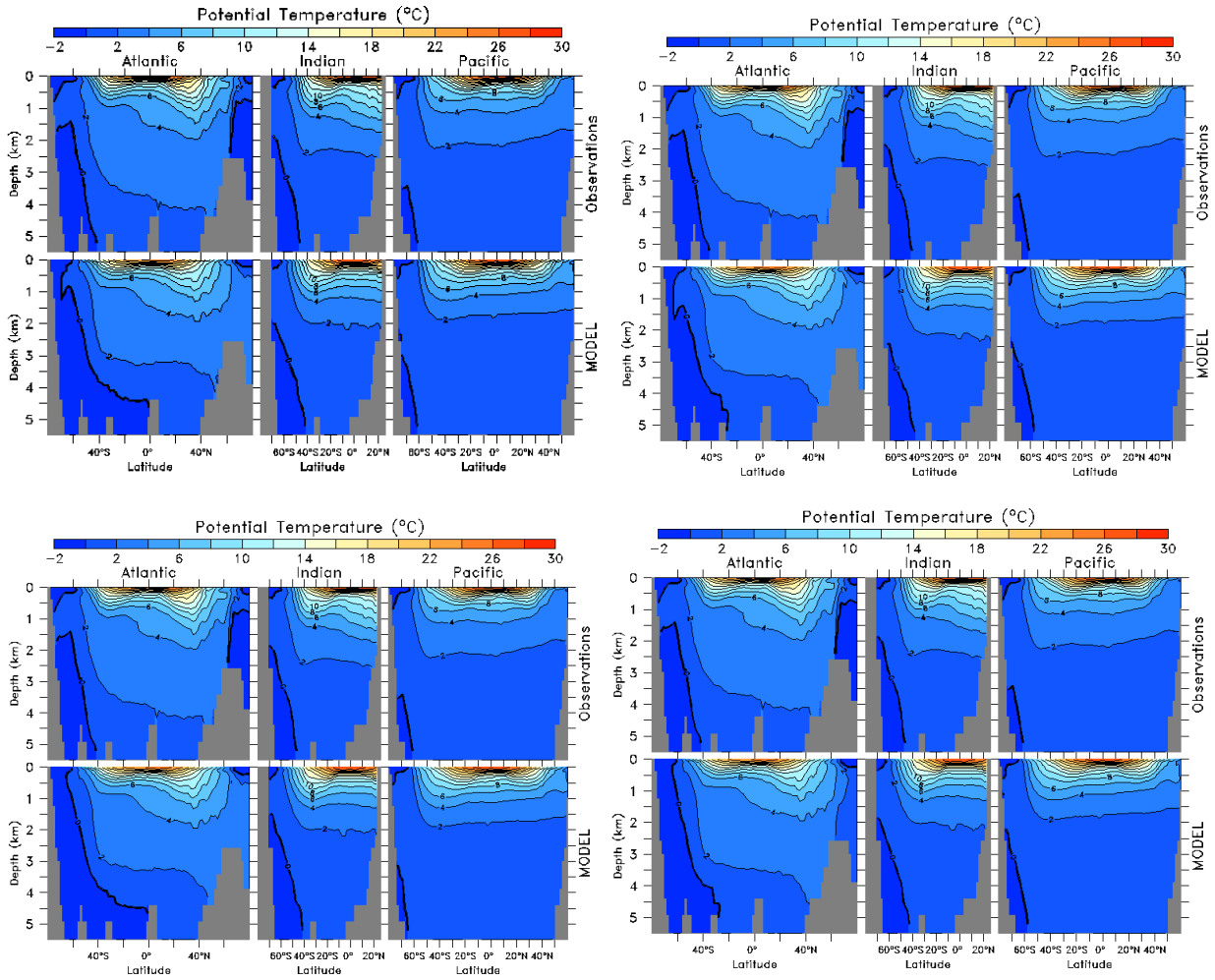

Figure 5. Pre-Industrial Potential Temperature (°C): Default (top left), Lower (top right), Middle (bottom left), Upper (bottom right)

As seen in Figure 5 (above), there is very little difference between the three parameter combinations and the default parameterization, especially in the Indian and Pacific Oceans. Comparing the different mixing efficiency parameterizations, *upper* yielded warmer temperatures, particularly in the deep Southern Ocean. *Default* and *lower* shared the same "hitch" of warmer temperatures in the Southern Ocean at a depth of 1 km while *middle* and

upper did not show this. Every parameter combination also shared warmer temperatures in the North Atlantic and there was little difference between them.

Temperature LGM:

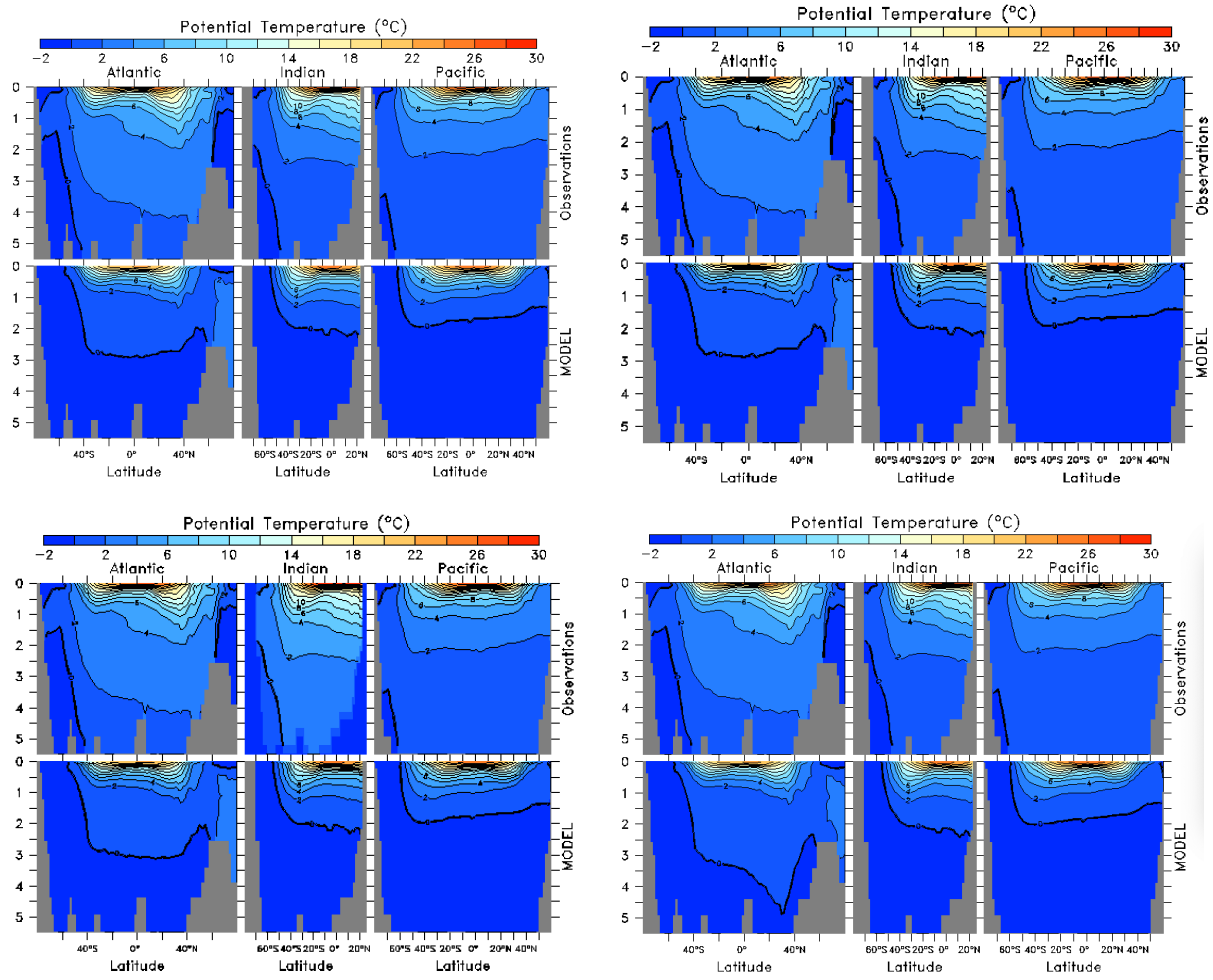

Figure 6. LGM Potential Temperature (°C): Default (top left), Lower (top right), Middle (bottom left), Upper (bottom right)

The simulation of the LGM ocean yielded temperature values that were very similar for lower parameters (*lower*, *middle*), and thus lower levels of mixing efficiency. The results for the *default* gamma were essentially identical to these two parameterizations. However, one difference was between the Atlantic Ocean in the *upper* simulation and all other simulations, the former of

which yielded higher temperatures in the deep ocean (~3-4.5 km) in the mid-latitude Northern Hemisphere. This area of the ocean corresponds to the region where relatively warm North Atlantic Deep Water (NADW) meets colder Antarctic Bottom Water (AABW). In the *upper* parameterization AABW flow between the equator and about 25N is reduced (see Figure 6), which leads to warming because of relatively more NADW influence.

C-14

C-14 Pre-Industrial:

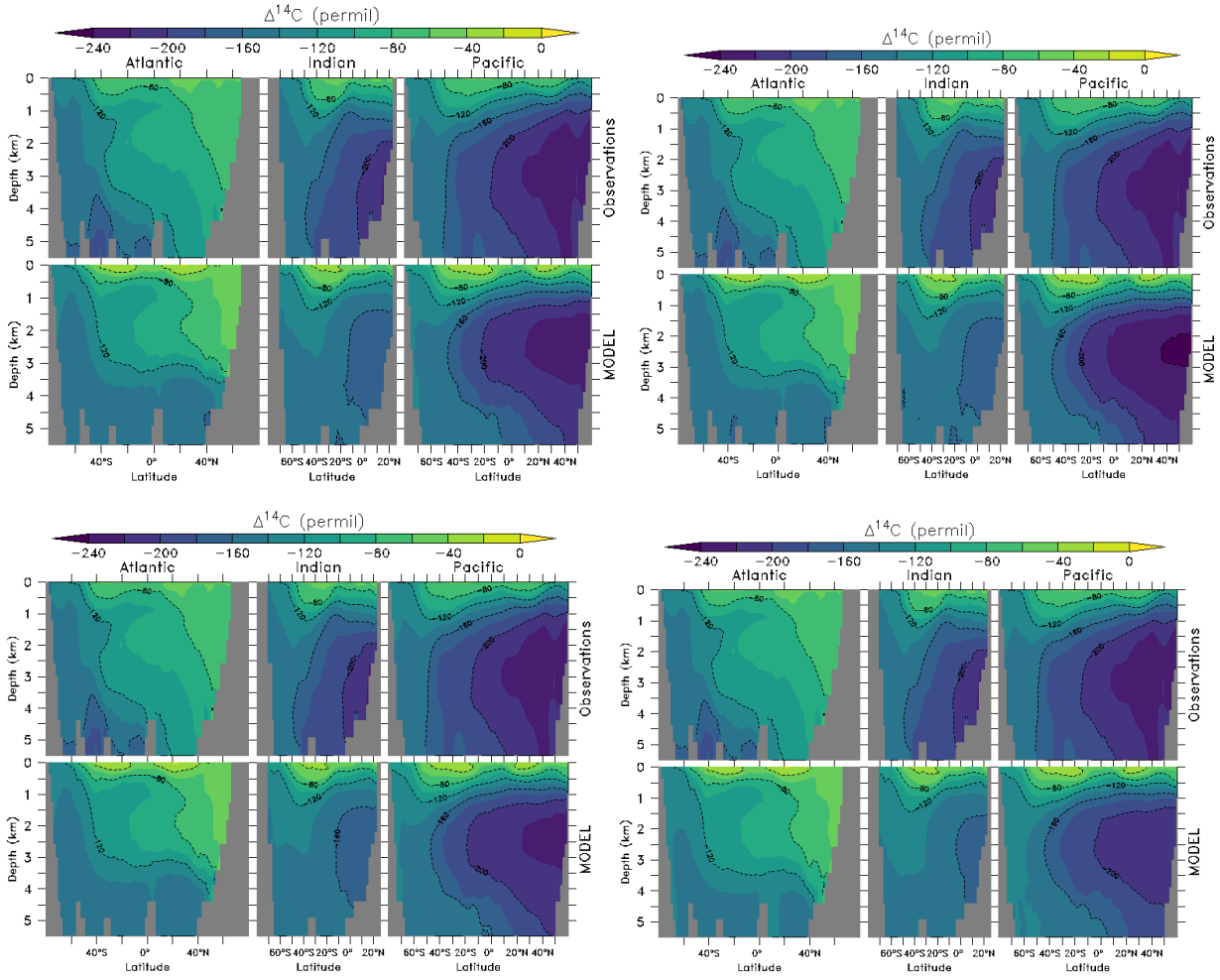

Figure 7. Pre-Industrial C-14 (ppt): Default (top left), Lower (top right), Middle (bottom left), Upper (bottom right)

Comparing C-14 Atlantic Ocean simulation outputs between the four parameter combinations, there is not much distinction between them, except for most of the deep ocean. Greater mixing efficiency, particularly with the *upper* parameterization, led to more positive $\delta^{14}C$ values throughout the deep ocean, due to larger volumes of NADW, which is high in $\delta^{14}C$, being able to reach below ~3 km. Water with C-14 levels of ~120 permil was able to reach roughly 500 m deeper in most latitudes of the deep ocean in the *upper* simulation than in any of the other simulations. At the surface, there was little to no difference between the parameter combinations, including the *default* simulation. The inclusion of a variable mixing efficiency made a difference in this ocean only with the *upper* parameter set. The same can be said with the Indian Ocean as well, where the *default, lower,* and *middle* simulation outputs again essentially approximating each other.

In the Pacific Ocean, there was more of a distinction in the C-14 levels between the different parameter sets. The most negative values are found in the North Pacific, because this water is the oldest in the World Ocean. $\delta^{14}C$ values there are higher in the *upper* case due to enhanced inflow of younger (high $\delta^{14}C$) waters from the Southern Ocean (Fig. 7). In all three oceans, the simulation outputs near the surface were near-identical and all had more positive $\delta^{14}C$ outputs (by ~20-40 permil) than the observations, but the observations there are influenced by uncertainties in removing anthropogenic effects. In short, most of the differences between *default* and the variable parameter sets were found in the deep ocean globally and in the middle depths of the Pacific. In general, the *default* results yielded C-14 levels in the Atlantic and Indian Oceans somewhat similar to the *lower* parameterization, whereas they were most similar to *middle* in the Pacific Ocean.

C-14 LGM:

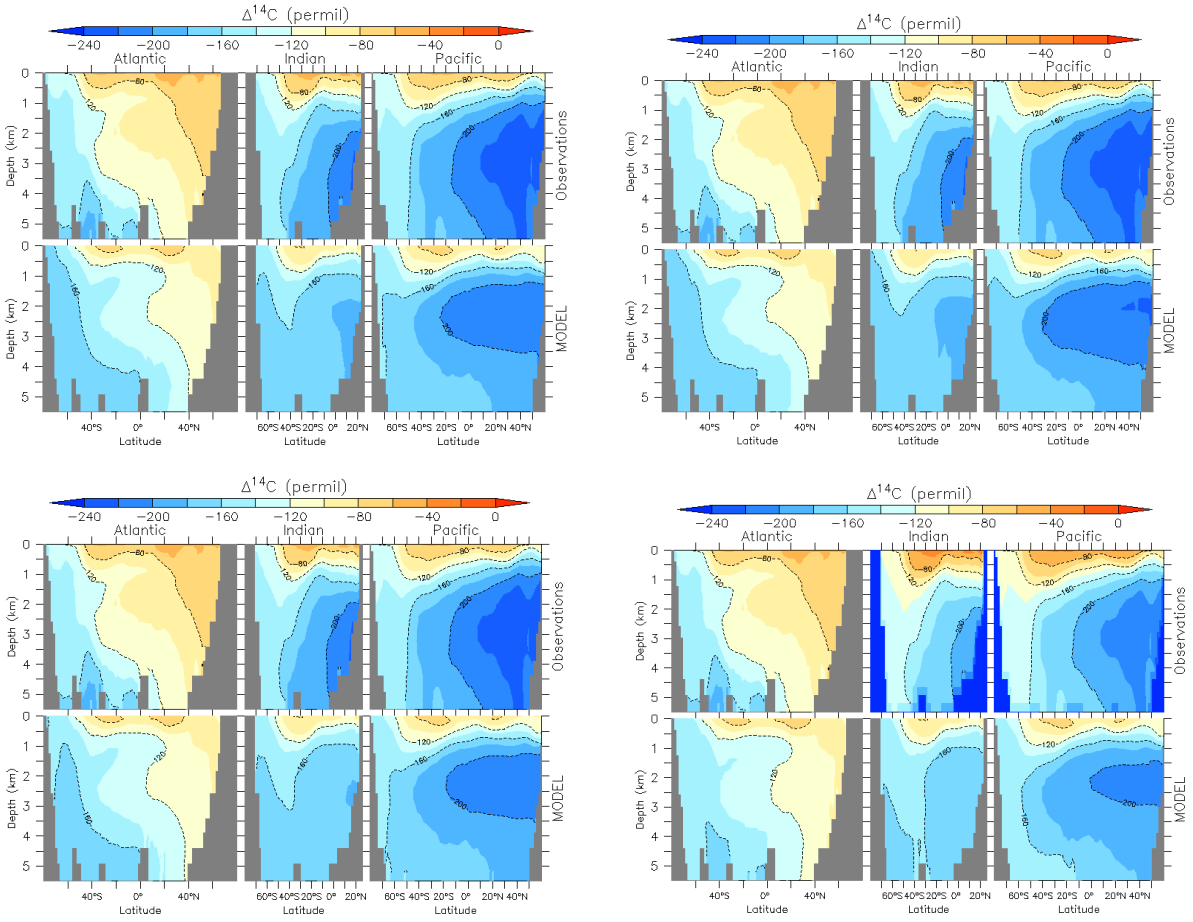

Figure 8. LGM C-14 (ppt): Default (top left), Lower (top right), Middle (bottom left), Upper (bottom right)

The simulation of C-14 in the LGM ocean showed that the general trend was that higher mixing efficiency parameters had more positive $\delta^{14}C$ values. For instance, in the *default*, *lower*, and *middle* simulations, most of the Southern Ocean was found to have a $\delta^{14}C$ in the -180 permil to -200 permil range while the *upper* simulation was in the -160 permil to -180 range. The *upper* results also show generally more positive C-14 values in the Indian and Pacific Oceans. Lastly, the constant mixing efficiency results were most closely approximate to the *lower* parameter results, but with slightly more positive permil values.

SALINITY:

Salinity Pre-Industrial:

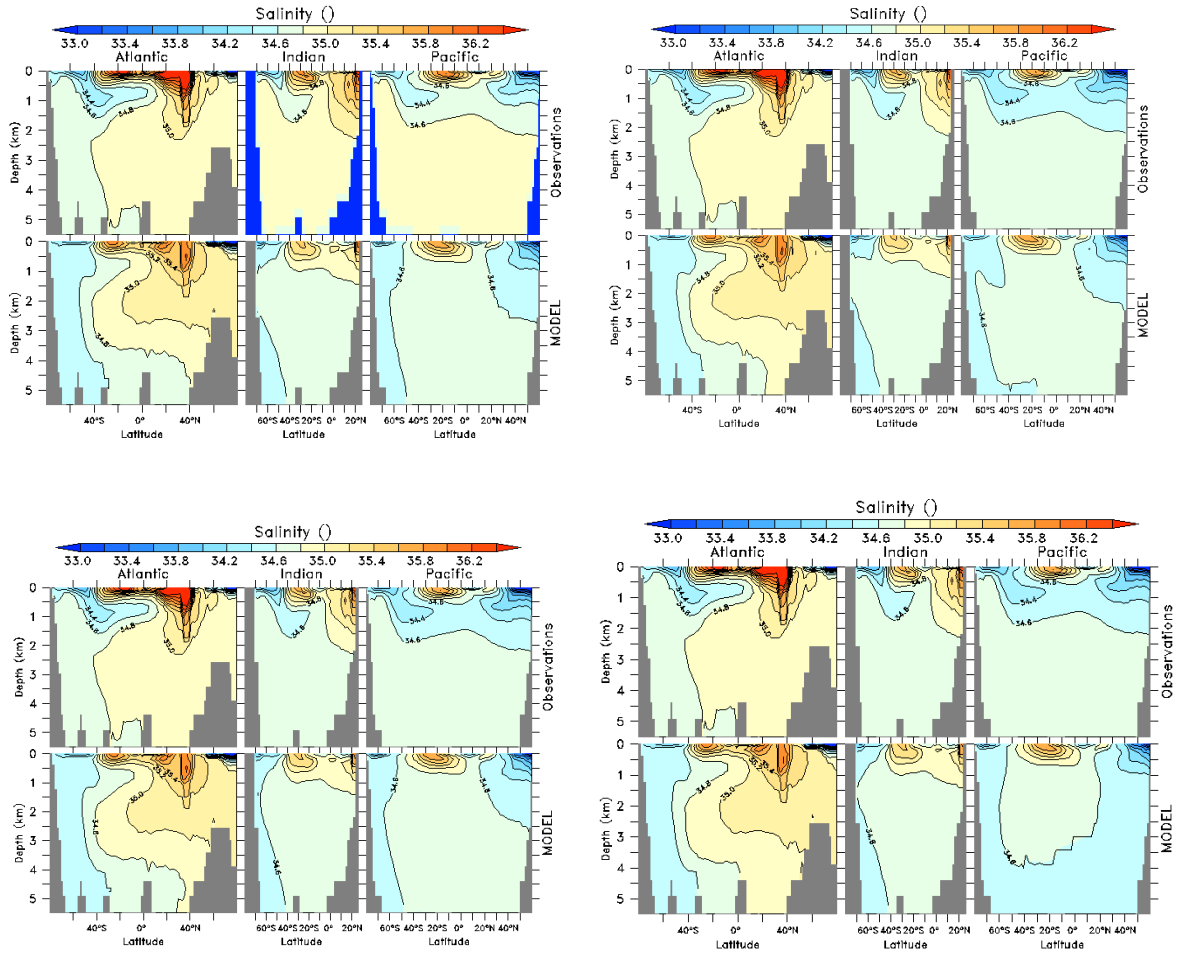

Figure 9. Pre-Industrial Salinity: Default (top left), Lower (top right), Middle (bottom left), Upper (bottom right)

The most significant differences between the default parameterization and three variable parameter conditions were in the Pacific Ocean, where the *upper* results yielded lower salinity values closer to the poles and in the deep ocean. This is likely because of increased northward advection of low salinity Antarctic Bottom Water (AABW) in the *upper* parameter combination. The outflow of low salinity Antarctic Intermediate Water (~34.4 ppt) from the

surface of the Southern Ocean (see Figure 9) that is seen in the observations jutting north into the Atlantic at about 0.5-1 km of depth is not as strongly represented in any of the parameter combinations, where it is shown as a weaker flow of water.

All four test cases underestimated the magnitude of salinity in the equatorial and subtropical Atlantic Ocean by roughly 0.5 ppt relative to the observations and more generally, the level of salinity throughout the ocean was lower than the observations. The relatively higher level of salinity in the Atlantic mid-latitudes captured the outflow of high salinity Medditeranean sea water as well as the greater levels of evaporation relative to precipitation. In general, there is not much difference between these parameter combinations and *default*, meaning changing the mixing efficiency likely has little effect on salinity results for the pre-industrial ocean.

Salinity LGM:

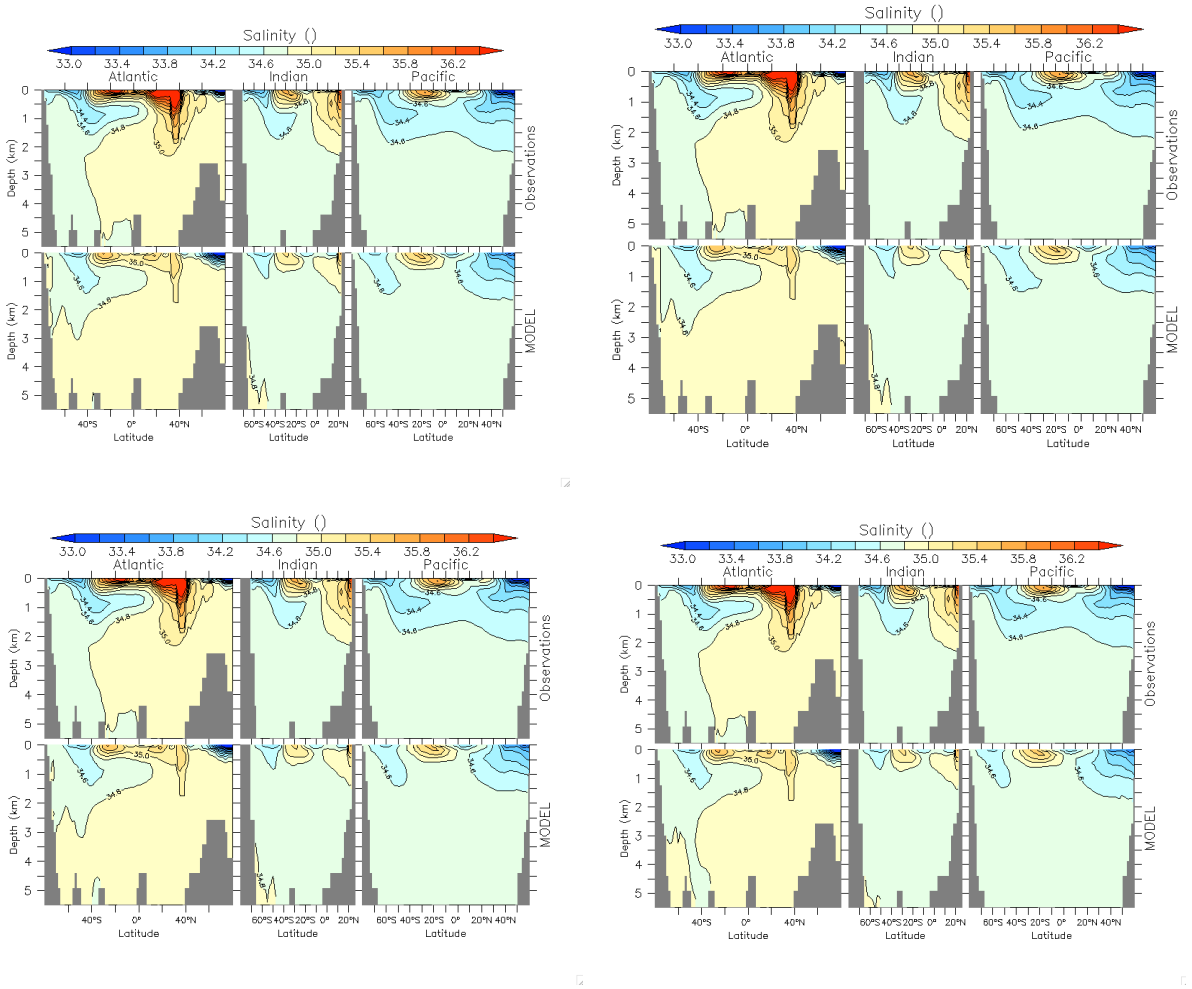

Figure 10. LGM Salinity: Default (top left), Lower (top right), Middle (bottom left), Upper (bottom right)

In Figure 10, elevated salinity values are present in the near-polar Southern Ocean for the *default*, *lower*, and *medium* simulations but not in the *upper* simulation. This uptick of salinity (around 0.2 ppt greater than the surrounding ocean) is most likely explained by brine rejection, i.e., the salt left behind by the freezing of sea ice. The greater mixing efficiency represented by the upper parameter may suggest that in this simulation, less sea ice was formed. In other parts of the LGM ocean, there was much less difference between the different parameter combinations.

CONCLUSIONS

We have explored the effect of a variable mixing efficiency on the state of the pre-industrial and LGM oceans. Specifically, we have tested the null hypothesis that there will be little difference between simulations run with a constant $\Gamma = 0.2$ and with the variable mixing efficiency parameterization. We find no significant effects of a variable mixing efficiency on differences between the physical ocean states of the pre-industrial and Last Glacial Maximum and therefore cannot reject the null hypothesis. This indicates that results obtained from previous simulations with a constant mixing efficiency are likely robust.

Another general finding was that the upper parameter condition of $(Re_b^*, \Gamma^*) = (300, 0.5)$ consistently output the strongest MOC results, no matter the ocean in question. This was expected, as this parameter combination results in the highest amounts of mixing, which drives MOC. The default runs yielded results that were typically between the medium and upper parameter conditions, but sometimes in between the lower and medium parameters (such as with salinity). This being said, it is unlikely that the variable Γ had a significant effect on MOC. For both the pre-industrial and LGM oceans, the difference between the *upper* parameterization and *default* were roughly 2 Sv, and there were no significant differences in the depth and shape of the AMOC (see Figures 1 and 2). The variable Γ also had little effect on other physical variables for both oceans. For future modeling, with limited computational resources in mind, a default mixing efficiency coefficient is suggested. However, future studies may be useful in further testing the effectiveness of a variable mixing efficiency.

REFERENCES

Gregg, M.C., D'Asaro, E.A., Riley, J.J., and Kunze, E. (2018). Mixing efficiency in the ocean. *Annual Review of Marine Science*. 10: p. 443-473, doi: https://doi.org/10.1146/annurev-marine-121916-063643.

Masheyek, A., H. Salehipour, D. Bouffard, C. P. Caulfield, R. Ferrari, M. Nikurashin, W. R. Peltier, and W. D. Smyth (2017). Efficiency of turbulent mixing in the abyssal ocean circulation. *Geophysical Research Letters, 44,* 6296-6306. doi:10.1002/2016GL072452.

MacKinnon, J.A., Z. Zhao, C.B. Whalen, A.F. Waterhouse, D.S. Trossman, O.M. Sun, L.C. St. Laurent, H.L. Simmons, K. Polzin, R. Pinkel, A. Pickering, N.J. Norton, J.D. Nash, R. Musgrave, L.M. Merchant, A.V. Melet, B. Mater, S. Legg, W.G. Large, E. Kunze, J.M. Klymak, M. Jochum, S.R. Jayne, R.W. Hallberg, S.M. Griffies, S. Diggs, G. Danabasoglu, E.P. Chassignet, M.C. Buijsman, F.O. Bryan, B.P. Briegleb, A. Barna, B.K. Arbic, J.K. Ansong, and M.H. Alford (2017). Climate Process Team on Internal Wave–Driven Ocean Mixing. *Bulletin of the American Meteorological Society*. 98(11): p. 2429-2454, doi: 10.1175/BAMS-D-16-0030.1.

Muglia, J. & A. Schmittner (2015). Glacial Atlantic overturning increased by wind stress in climate models. *Geophysical Research Letters, 42,* 1-8. doi:10.1002/2015GL064583.

Muglia, J., L.C. Skinner, and A. Schmittner (2018). Weak overturning circulation and high Southern Ocean nutrient utilization maximized glacial ocean carbon. Earth and Planetary Science Letters. 496: p. 47-56, doi: 10.1016/j.epsl.2018.05.038.

Schmittner, A. and G.D. Egbert (2014). An improved parameterization of tidal mixing for ocean

models. Geoscientific Model Development. 7(1): p. 211-224, doi: 10.5194/gmd-7-211-2014.

Sherriff-Tadano, et al. (2017). Influence of glacial ice sheets on the Atlantic meridional overturning circulation through surface wind change. *Climate Dynamics, 50*, 2881-2903. DOI 10.1007/s00382-017-3780-0.

Smyth (2020) Marginal Instability and the Efficiency of Ocean Mixing, *J. Phys. Oceanogr.* 50, 2141, DOI: 10.1175/JPO-D-20-0083.1.

St. Laurent, L. C., Simmons, H. L., and S. R. Jayne (2002) Estimating tidally driven mixing in the deep ocean, *Geophys. Res. Lett.* 29(23), 2106, doi:10.1029/2002GL015633.

Weaver, A. J., M. Eby , E. C. Wiebe , C. M. Bitz , Phil B. Duffy , T. L. Ewen, A. F. Fanning , M. M. Holland , A. MacFadyen , H. D. Matthews , K. J. Meissner , O. Saenko , A. Schmittner , H. Wang & M. Yoshimori (2001) The UVic earth system climate model: Model description, climatology, and applications to past, present and future climates, *Atmosphere-Ocean*, 39:4, 361-428, DOI: 10.1080/07055900.2001.9649686

Wilmes, S. B., A. Schmittner, J. A. M. Green (2019). Glacial ice sheet extent effects on tidal mixing and the global overturning circulation. *Paleooceanography & Paleoclimatology*, 34(8). https://doi.org/10.1029/2019PA003644.